Geologie en Mijnbouw 66: 21–34 (1987)

Gravel- to sand-sized vivianite components in a Saalian till layer near Borne (The Netherlands)

P.A. Riezebos[1] and M. Rappol[2]
[1] *Laboratory of Physical Geography and Soil Science, University of Amsterdam, Dapperstraat 115, 1093 BS Amsterdam, The Netherlands;* [2] *Terrain Sciences Division, Geological Survey of Canada, 601 Booth Street, Ottawa, Ontario, Canada*

Received 22 September 1986; accepted in revised form 23 January 1987

Abstract

Vivianite particles have been found within the gravel and sand fractions of a specific level of a Saalian till layer. Besides with gravel constituents, which are common in Dutch till deposits, the vivianite granules are associated with sedimentary rock fragments containing a.o. glauconite and a kind of phosphoritic grains that are cemented by carbonates. The vivianite aggregates can be observed inside this carbonate matrix. Individual vivianite granules were studied in thin section and by SEM, X-ray diffraction, microprobe and differential thermal analyses. Only the monoclinic phase of $Fe_3(PO_4)2.8H_2O$ could be established with certainty. The vivianite of the granules contains lower Ca, Mn, Mg, Si and Al abundances than the vivianite of the aggregates included in the carbonate matrix. It is concluded that the vivianite granules are of non-detrital origin.

Introduction

Vivianite occurrences in the Netherlands are mainly restricted to sediments and associated fossils of Holocene age (Van Bemmelen, 1896; Van Baren, 1927; De Smet, 1962; Zwaan & Kortenbout van der Sluys, 1971). Van Calker (1885), however, reported 5–7 mm long vivianite crystals on a mammoth molar, which was found in SE Drente nearly 5 m below the surface under a cover of sand and peat. In view of the kind of fossil the vivianite was associated with, Van Calkers find might represent the only reported occurrence in Dutch pre-Holocene deposits.

In the course of a petrological description of samples from a temporarily exposed Saalian till near the village of Borne (Fig. 1), blue-coloured vivianite nodules were observed in the 2–5 mm gravel fraction (Fig. 3A). Their rounded to sub-rounded form is in contrast with the shape of the other constituents in that size range. The earthy and rather delicate nature of these granules became evident during pretreatment of the sample material, when slight crushing produced a dark-bluish staining powder. Henderson et al. (1984) reported that in New-Zealand vivianite was used by the Maori for pigment.

Vivianite, $Fe_3(PO_4)_2 \cdot 8H_2O$ is one of the most common hydrated ferrous phosphate minerals. Its origin is usually associated with anoxic environments where iron and phosphate is available in sufficient quantity, and where the formation of pyrite is inhibited by low sulphide activities (Nriagu, 1972). Hence it is frequently observed in peat, lake and estuarine deposits, also in close connection with bone and wood fragments in these sediments (Hearn et al., 1983, and references cited therein). As secondary mineral it is found in the

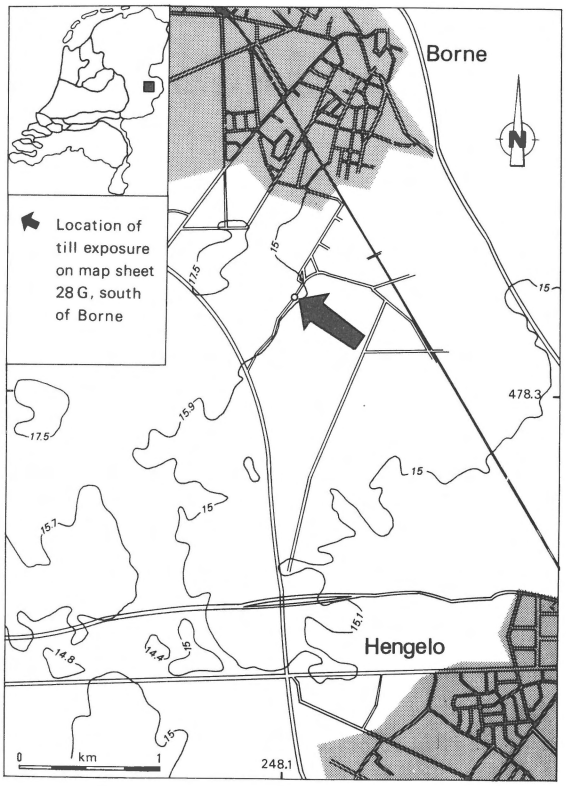

Fig. 1. Map showing the site of the excavation.

gossans of metallic ore deposits, in weathering products of primary phosphates (o.a. Anderson et al., 1962), and even as film-like coatings on phosphates in several iron meteorites. The mineral has also been reported in the Middle Eocene green sands of the Aquia Formation, Maryland (Barwick, 1951).

During the last two decades many investigations have been devoted to the study of the basic hydrated phosphates. Much attention was paid not only to their crystal chemistry (Moore, 1965a and b, 1970a and b, 1971) in order to understand their mineralogical and petrological properties, but also to their natural occurrences and the processes involved in their formation in freshwater environments (Shimada & Kono, 1971; Bray et al., 1973; Dell, 1973; Rosenquist, 1970; Nriagu, 1972; Nriagu & Dell, 1974; Emerson & Widmer, 1978; Rodgers, 1977; Henderson et al., 1983, 1984). Precipitation and dissolution of these mineral phases may be a mechanism regulating the P contents in freshwater systems and as such they may be of interest in understanding and solving eutrophication problems.

Therefore a closer study of the vivianite nodules seemed worthwhile, also because their present occurrence raises the question whether the vivianite originated before, during or after the formation of the till layer. It is well known that in the eastern Netherlands detrital material from the underlying. Tertiary is abundantly present in the recognized glacial deposits. There is some doubt, however, whether the marginal zone of an ice sheet between the ice/till and till/substratum interfaces is the most favourable environment for vivianite formation. On the other hand, if the necessary conditions for an authigenic origin are met, a post-depositional formation in any type of environment seems possible.

In this paper a closer examination of this vivianite and also of another, rather uncommon, associated gravel constituent is reported.

Location and setting of the till layer

The till was exposed in an excavation for a tunnel construction south of the village of Borne (Fig. 1). It's stratigraphical position is discussed by Van der Meene (1984). The till is underlain by the Formation of Rupel (Tertiary) and overlain by eolian and locally running-water sands of the Formation of Twente (Weichselian). Van der Meene (1984) also recognized Tertiary rock fragments in the till bed.

At the sampling site the overlying sands have a thickness of 5 m and show a subhorizontal stratification. The upper portion of the at least 2.5 m thick till bed was disturbed, and some mixing with the covering sands was noticeable. At other localities Van der Meene (1984) noticed a concentration of gravels and boulders ("lag deposit") at the till/sand boundary, which indicates rather severe erosion of the till after its accumulation.

At five levels in the till bed (see Fig. 2 for depths) material was collected for petrographical and grain-size analyses. This sampling was done within the framework of a study of the Dutch till deposits

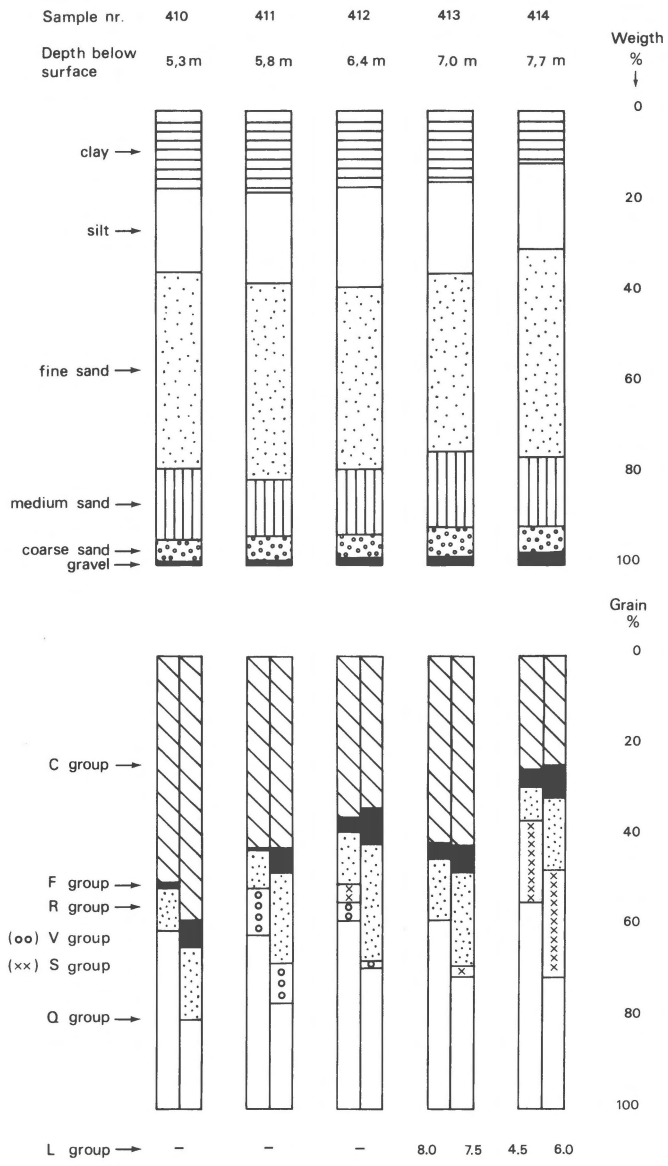

Fig. 2. Size distributions and petrological compositions of the 2–3 mm (left bar) and 3–5 mm (right bar) gravel fractions. For explanation of the petrological groups cf. text. Only the L group is expressed as a percentage of all groups.

(Rappol, 1983, 1984). Samples 414 and 413 were obtained with an auger as the lower part of the till was not exposed at the sampling site.

Experimental

The bulk samples were dried at 60° C and mechanically disintegrated. The gravel was separated from the < 2 mm material by dry sieving, subsequently washed and isolated in separate sieve fractions. Grain-size distributions of the < 2 mm material were established by applying a combination of sieving (sand fraction) and pipette analysis (silt and clay fractions). Several size-grades obtained were examined using a binocular or a petrological microscope.

Following Zandstra (1978), a number of rock-

groups were determined in the 2–3 mm and 3–5 mm gravel fractions, viz: a C group (igneous and metamorphic), an F group (angular flint), a Q group (quartz), and L group (limestone and calcareous) and an R group (restgroup, mainly comprising sedimentary rock types). Since this R group contained relatively high percentages of vivianite nodules and a particular kind of sandstone fragments, two groups were added to Zandstra's scheme, an S group (brown sandstone fragments) and a V group (vivianite nodules).

Individual specimens from these S and V groups were thin-sectioned for microscopical examination. Fresh fragments of crushed vivianite granules were studied with the SEM (I.S.I. DS 130). Powdered single vivianite granules were subjected to differential thermal analysis (Linseis L 62 two channel recorder; DTA channel: 50 μV F.S.; T channel: 10 mV F.S.) and X-ray diffraction analysis (Guinier de Wolff camera, FR 552). Finally, thin-sectioned vivianite nodules and sandstone granules were polished, carbon-coated and subjected to electron microprobe analysis (Microscan 9, Cambridge Instruments). Standards listed in Table 1 were employed and percentages were corrected (ZAF-corrections) by an on-line computer program provided by the manufacturer. The electron microprobe analyses were performed at the Instituut voor Aardwetenschappen, Vrije Universiteit, with financial and personnel support by Z.W.O. – W.A.C.O.M. (research group for analytic chemistry of minerals and rocks, subsidized by the Netherlands Organisation for the Advancement of Pure Scientific Research).

Results

Grain-size distributions and gravel petrography

Figure 2 displays that the grain-size distributions are rather similar and give hardly occasion to differentiate the till bed in subunits. Only the lowermost sample (414) has a comparatively low clay content.

More variation is shown in the petrological composition of the gravel components. The C group increases upwards in the section, suggesting a growing share of northern material in the otherwise, in weight, scanty gravel fractions. The F group, however, decreases towards the top of the till, a feature fairly common in southeast Drenthe (Rappol, 1984). Members of the L group were only observed in the lowermost samples. In the basal sample the S group is conspicuously abundant. Likewise the sudden appearance of the V group at a higher level in the till bed contributes to this variation. A visual estimate of vivianite particle density in the associated sand fractions of sample 411 suggests their presence in measurable quantities in the size grades > 2 phi (Plate 2F), but they seem to be almost lacking in the smaller size fractions.

Morphology and fabric of individual vivianite nodules

Figure 3A shows that the nodule surface have irregular cavities, which suggests an internal cavernous structure. Figures 3B and 3C demonstrate that voids which vary in size and shape are indeed present, but not in such a degree that the term "cavernous" seems appropriate. These voids are mostly

Table 1. Standards used for quantitative electron microprobe analysis.

Na	–	jadeite	S	–	barite	Cr	–	chromium oxide
Mg	–	olivine	Cl	–	halite	Mn	–	rhodonite
Al	–	corundum	K	–	orthoclase	Fe	–	hematite
Si	–	diopside	Ca	–	diopside	Ni	–	nickel oxide
P	–	apatite	Ti	–	ilmenite			

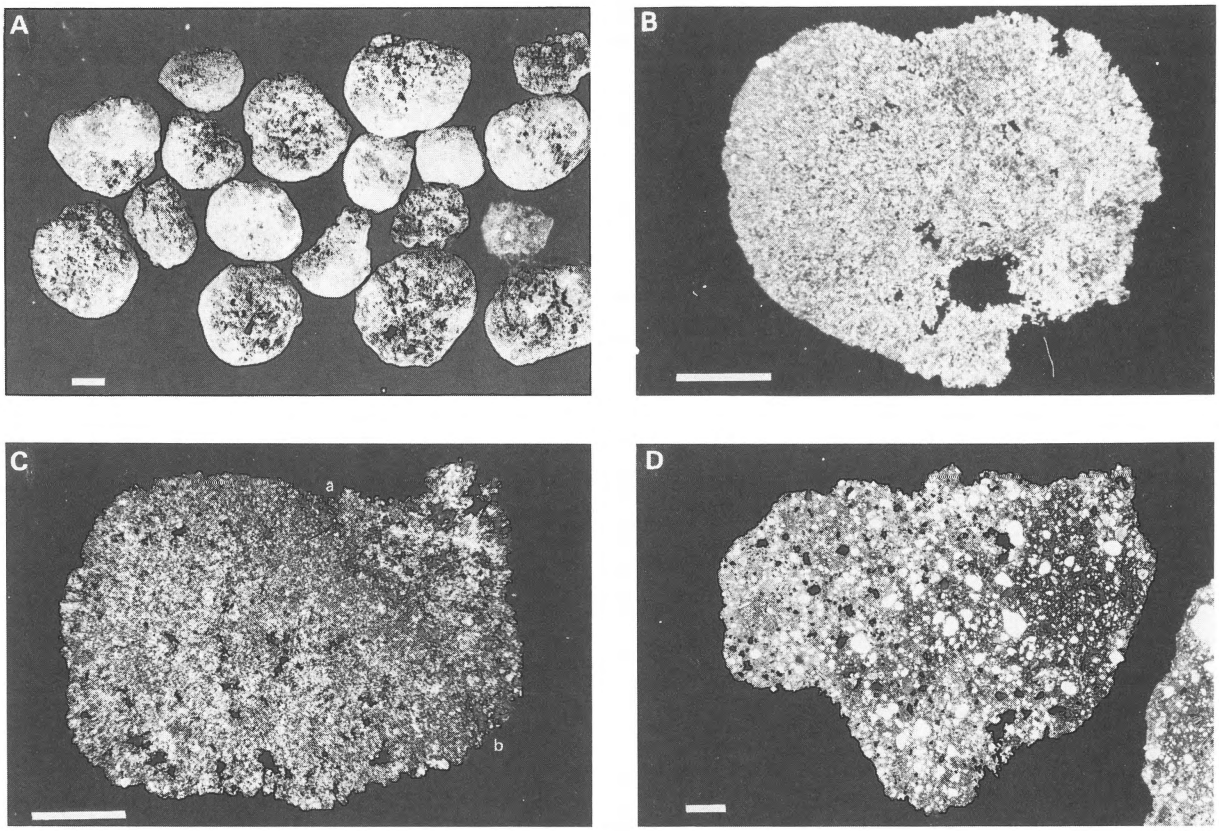

Fig. 3. A. Vivianite nodules in oblique incident light. B and C. Thin-sectioned vivianite nodules (crossed polarizers). D. Thin-sectioned granule of the S group (crossed polarizers). Bars indicate 1 mm.

empty (Fig. 3B and C), although bigger ones may contain one or a few single mineral particles. Occasionally small amounts of isotropic, grey-brown to brown-black (organic?) matter was observed as a partial infill.

In spite of the pretreatment washings, a coating of yellow-brown clayish material locally still adheres to the nodule surfaces. This is, however, not visible in Figures 3B and C, but higher magnifications and the use of colour film make it clear (Plate 1A). It is particularly common in surface depressions, and this clayey substance may contain individual sand-sized mineral particles such as quartz and glauconite. Inclusion of the clayish material within the vivianite mass, has only been noticed once, and appeared to be a discontinuous vein (plane?) connecting two opposite surface cavities (see a–b in Figure 3C).

The vivianite groundmass is crypto- to microcrystalline (Fig. 4B and D, Plate 1D) with mostly subhedral to euhedral constituents. In plane-polarized light their pleochroic colours vary between dark cobalt blue and pale olive-green to yellow (Plate 1B). Several crystallites fail to display clear pleochroism or exhibit blue green instead of cobalt blue colours. Microcrystalline domains with radial and bush-shaped patterns (Plate 1B and C) are often discernable. Rather abrupt transitions from crystalline to adjacent cryptocrystalline areas with a more random orientation of smaller and more equigranular constituents facilitate their recognition (Plate 1D and E). The larger crystals in the patterns mentioned display a columnar habit and are more or less neatly arranged in fibres. According to their pleochroic scheme, the crystals mainly developed parallel to [001] and seem to be stuck on

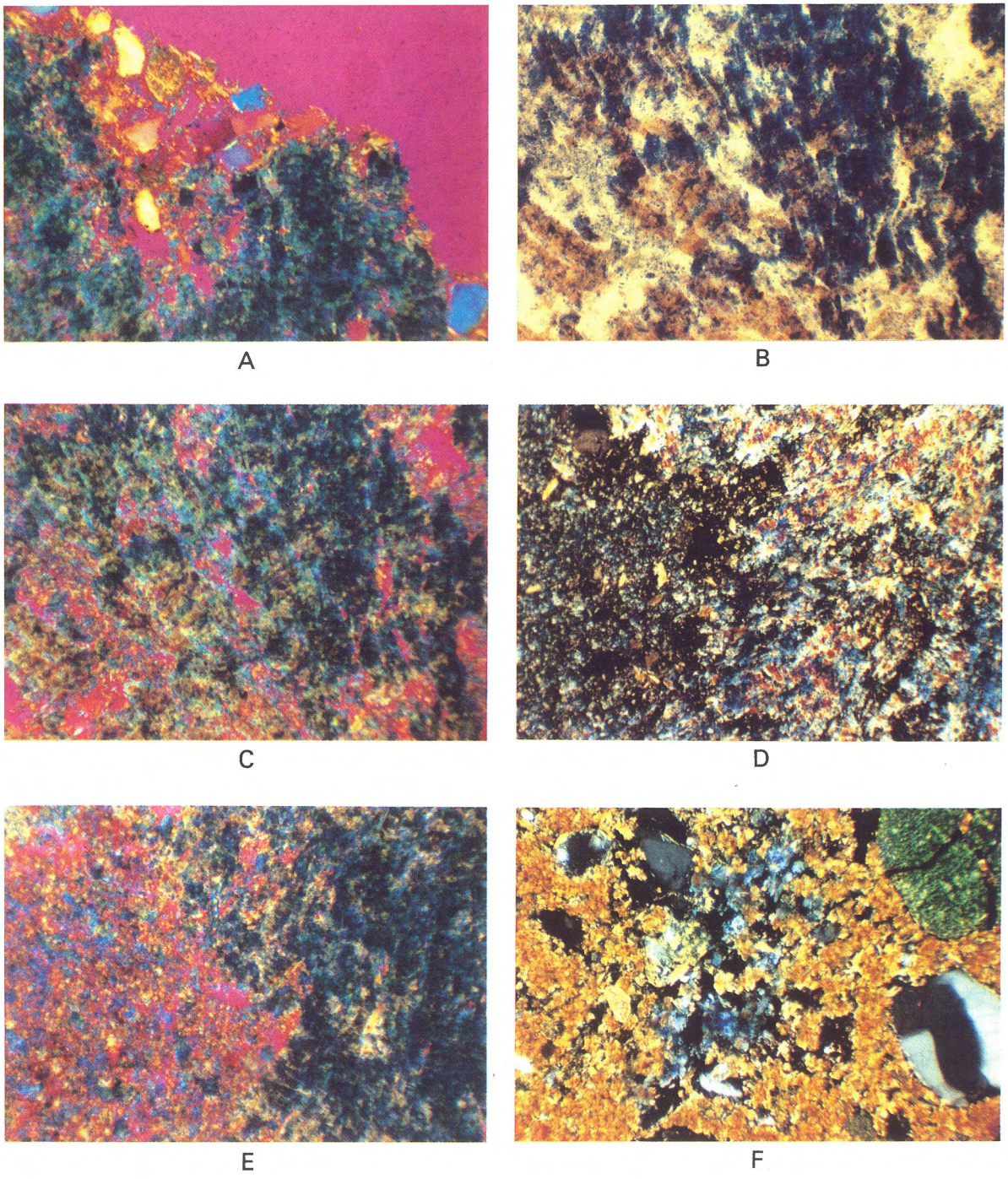

Plate 1. (A) Surface depression of vivianite nodule filled by till material. Crossed polarizers + gypsum, magnification 277 ×. (B) Bush-shaped arrangement of vivianite crystals in nodule. Plane-polarized light, magnification 277 ×. (C) View of B under crossed polarizers + gypsum plate. (D) Abrupt transition in crystallinity inside a 2–3 mm vivianite granule. Note in the top left hand corner the partial infill of a pore by a mineral grain. Crossed polarizers, magnification 322 ×. (E) Another example in a 3–5 mm nodule. Crossed polarizers + gypsum, magnification 322 ×. (F) Cluster of vivianite crystals in microcrystalline carbonate matrix of a member of the S group. Crossed polarizers, magnification 277 ×.

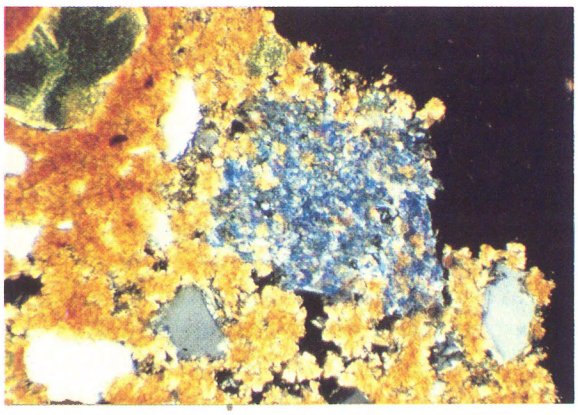

A

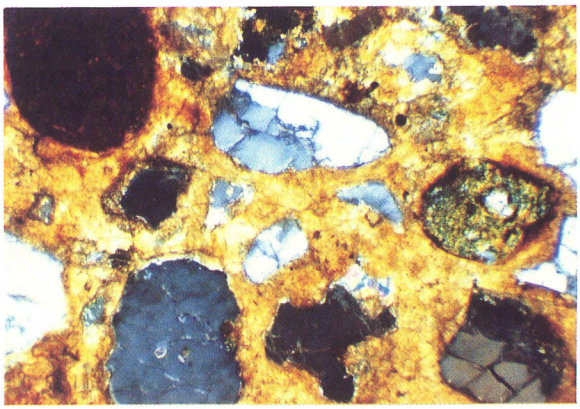

B

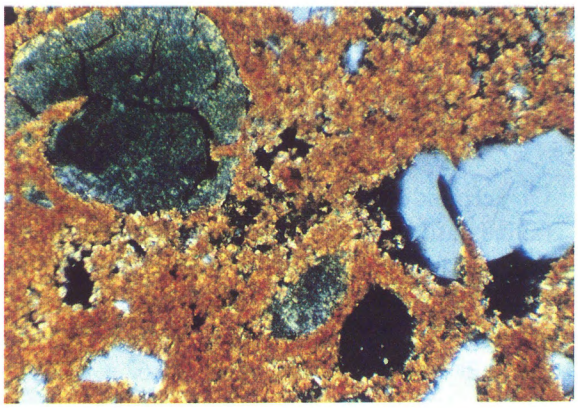

C

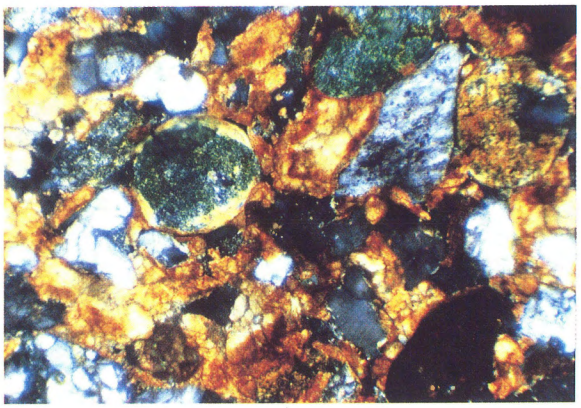

D

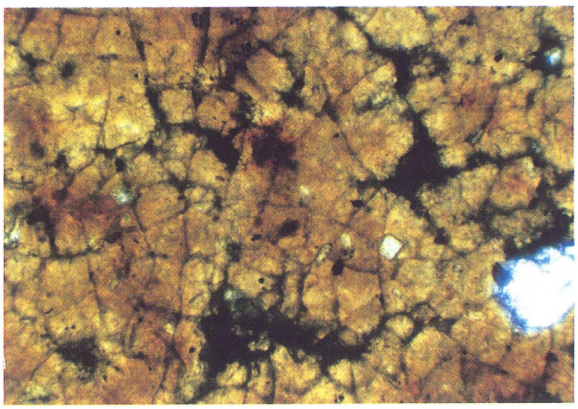

E

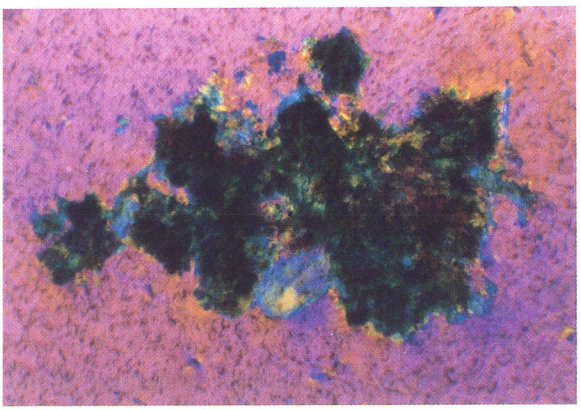

F

Plate 2. (A) Vivianite cluster occurring in the marginal zone of an S granule. Note the glauconite grain with crack development. Crossed polarizers, magnification 277 ×. (B) Thin-sectioned S granule showing cracked quartz particles. In upper left-hand corner a brown isotropic pellet. Crossed polarizers, magnification 277 ×. (C) Thin-section of S granule with predominating carbonate matrix. Note the crack infill of the glauconite pellet. Crossed polarizers, magnification 277 ×. (D) Polished thin-section of S granule with a high density of framework particles. Crossed polarizers, magnification 277 ×. (E) Polished thin-section of S granule consisting mainly of calcareous mud. Interstitial spaces (here black) are sometimes filles with micrite. Plane-polarized light, magnification 277 ×. (F) Thin-sectioned vivianite sand particle from the 1–2 phi size range. Crossed polarizers + gypsum plate, magnification 322 ×.

the (010) and (110) faces in the direction of the fibre axes.

Figure 4A shows a freshly broken fragment from a 3–5 mm vivianite nodule, and higher magnifications of the broken surface (Figure 4B, C and D) provide a better three-dimensional illustration of the fabric. These SEM images also indicate that several crystallites display a tabular to platy habit.

Morphology and fabric of individual S group members

Owing to their presence at the basal and the vivianite-bearing levels, the members of the S group have been examined more closely. In contrast with the members of the V group, they have a more angular and more irregular shape (Fig. 3D). Thin-section analyses reveal that they are fragments of sedimentary rocks. Quartz, felspar particles, glauconitic and brown isotropic pellets are the most common framework constituents (Plate 2, B, C, and D). In a few specimens lithoclasts were occasionally observed. The framework constituents occur in varying proportions and are cemented by a microcrystalline carbonate matrix. Some of the thin-sectioned S granules appear to consist primarily of brown calcareous mud with only a few widely dispersed grains of the constituents mentioned (Plate 2E). The mud shows curious desiccation patterns. Such S granules might be classified as remnants of calcareous mudstones or wacke stones. The others with more abundant framework particles very probably derive from calcareous, glauconitic and/or phosphoritic sandstones, although in view of their low packing density (Kahn, 1956) the term wacke might be better justified (compare e.g. Plate 1F, Plate 2B, C and D).

Quartz occurs as mono- to polycrystalline, angular to rounded grains with occasionally undulating extinction and clear "embayment" features. Angular grains abundantly display internal cracks (Plate 2B). Several of the felspar particles, which may have fresh and "weathered" appearances, show polysynthetic twinning. The glauconitic constituents are mostly rounded and may also be cracked (Plate 2A and C). Occasionally, the cracks are filled with carbonate crystallites. The dark brown isotropic grains, which in general attain the largest dimensions, may likewise show cracks. Their mineralogical nature, however, could not be assessed under the microscope. Microprobe analysis (see Table 3) indicates that they consist largely of Ca phosphate and hence, they are probably sand-sized phosphorite grains. The SEM views of a freshly broken surface of a glauconitic sandstone fragment illustrate their internal structure (Fig. 4E and F).

In four out of twelve thin-sectioned S granules, the calcareous matrix appeared to contain one or more clusters of vivianite crystals (Plate 1F, Plate 2A). The dimensions of these aggregates or clusters did not exceed 1 phi.

X-ray diffraction data of the vivianite nodules

On account of the dominant micro- to cryptocrystalline nature of the vivianite granules, single crystals could not be studied. A complete powder pattern obtained from some crushed Borne vivianite granules is presented in Table 2 and compared with the data on the ASTM card 30 – 662 + 662A.

A general agreement between the two patterns is undeniable, be it that the Borne vivianite has some more reflections. Moreover, there is a clear distinction in the estimated intensities of the corresponding reflections. The present ASTM vivianite (card 30–662) replaces card 3–70 and the pattern of the latter showed a considerably lower number of reflections, but a better conformity in the intensities of the corresponding lines.

A mixture of non- or less iron-containing analogues of monoclinic and triclinic polymorphs (with their close similarity in lattice) might explain the difference. Some insignificant lines in the Borne pattern, e.g. 3.64, 3.04 and 2.80 Å might be attributed to metavivianite, but a more prominent one of this triclinic phase (8.59 Å is absent in the Borne pattern, while the other important lines, 6.71, 4.86 and 3.87 Å, are very close in position to the strongest vivianite reflections (see table 1 in Ritz et al., 1974). Furthermore, the position of the majority of the most prominent reflections in the Borne vivianite pattern (7.93, 6.72, 3.85, 3.20,

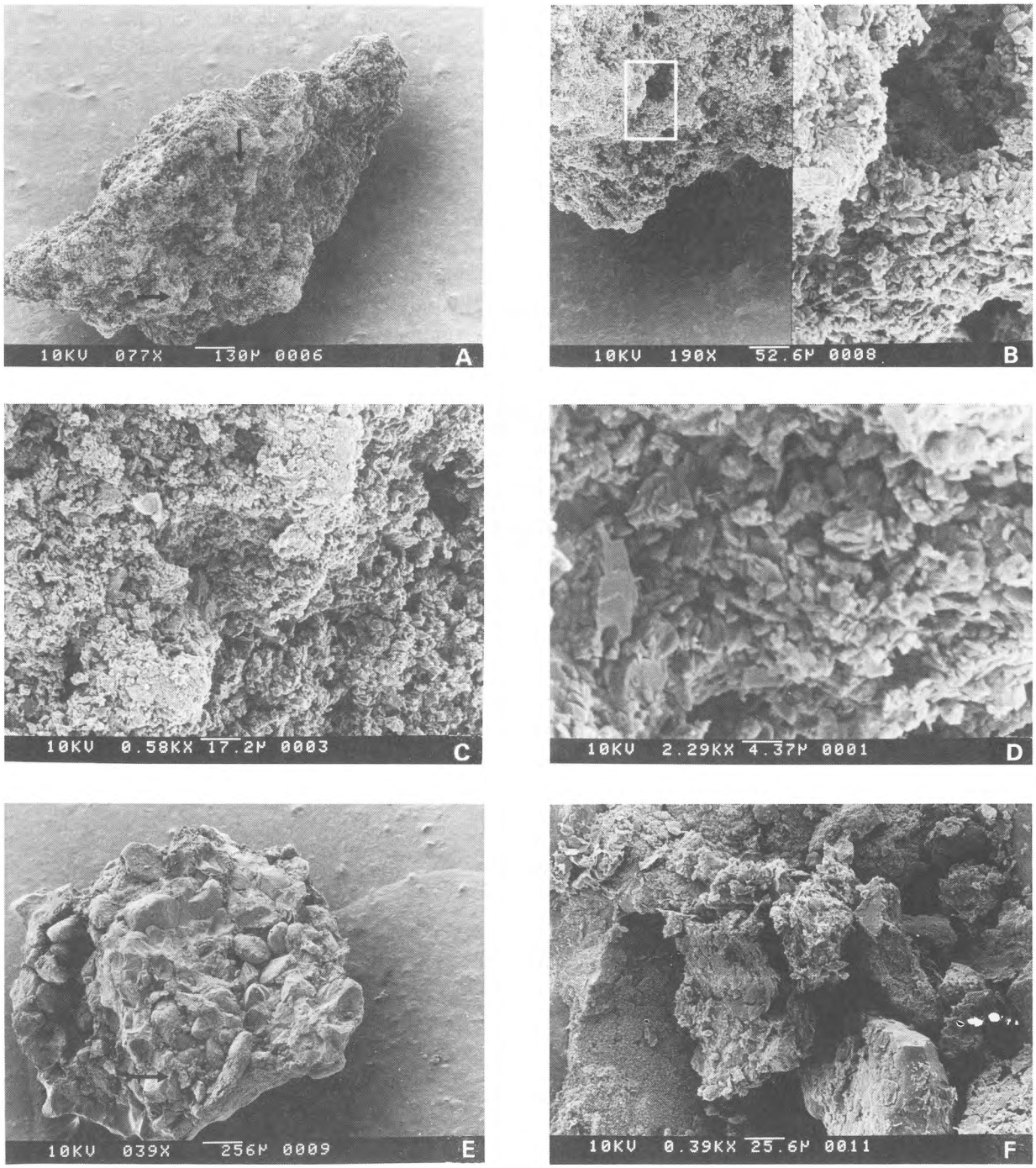

Fig. 4. Scanning-electron micrographs showing fresh fractures of fragments obtained by crushing a V group member (A, B, C and D) and an S group member (E and F). The lower arrow in A indicates the close-ups in B, the upper one the enlarged area C. D is the magnified central portion of C. In F (see arrow in E) locally arrangements of crystallites are discernable, which are rather similar to those shown by the vivianite (see e.g. top left hand corner).

2.963 and 2.70 Å) corresponds more or less with the strongest lines in the pattern of baricite (see table 3 in Sturman & Mandarino, 1976).

In any case, the Borne vivianite pattern seems to illustrate that it is rather difficult to discriminate between monoclinic vivianite and possible other related mineral phases merely on the basis of conventional X-ray diffraction techniques.

Differential thermal analysis

The DTA curve of the Borne vivianite was obtained under the following conditions: 15 mg crushed material ($<2\,\mu m$) mixed with 40 mg Al_2O_3 and the sample was tamped; reference material: 60 mg annealed Al_2O_3 ($<2\,\mu m$); heating rate: 10° C/min; sample holders were platinum sleeves (0.17 cm^3), dimension: 10 × 35 mm ∅.

The curve in Fig. 5 shows to distinct exothermal peaks, at 676° and 758° C, and a weak one at 316° C. An endothermic reaction is further clearly visible within the 60–200° C range and is the result of dehydration. This reaction apparently reached a maximum at 148° C, but small subpeaks at ca. 182° and ca. 120° C suggest that this event is a little more complex.

Table 2. X-ray powder diffraction data of the Borne vivianite (Guinier camera FR 552; 229.2 mm ø, Co K radiation; Johansson monochromator). For comparison ASTM data have also been presented.

Vivianite (Borne)		Vivianite (Astm. 30–662)		Vivianite (Borne)		Vivianite (Astm. 30–662)	
d (A°)	I	d (A°)	I	d (A°)	I	d (A°)	I
7.93	79	7.93	13	2.170	16	2.173	2
6.72	100	6.73	100	2.154	5		
4.90	67	4.900	12	2.106	10	2.108	1
4.55	41	4.558	5	2.075	20	2.075	4
4.34	29	4.341	2	2.032	2	2.039	<1
4.07	23	4.081	12	2.008	4	2.012	2
3.85	69	3.849	7	1.969	13	1.964	2
		3.768	<1	1.938	10	1.936	2
3.64	18			1.933	2		
		3.361	1	1.924	42		
3.34	32	3.343	2	1.902	19		
3.20	71	3.210	16	1.889	16	1.886	2
3.17	20			1.882	7		
3.04	4			1.818	15	1.816	2
2.975	74	2.985	10	1.794	4	1.793	1
2.963	65	2.960	8	1.783	8	1.786	3
2.804	12			1.768	8	1.772	2
		2.770	4	1.679	15	1.6809	6
2.724	64	2.728	9	1.670	31		
2.700	46	2.706	9	1.655	18	1.6599	2
2.639	26	2.637	6	1.632	8		
2.590	6	2.593	4	1.597	17	1.5974	3
2.529	45	2.530	8	1.587	17		
2.513	21	2.514	3	1.582	15	1.5834	4
2.449	8	2.448	1	1.561	3		
2.424	53	2.421	6	1.551	7		
2.346	3			1.538	3	1.5404	1
2.315	26	2.321	7	1.518	18		
2.281	16	2.296	1	1.499	10		
		2.279	1	1.490	13		
		2.233	5	1.470	3		
2.188	18	2.194	5	1.462	5		

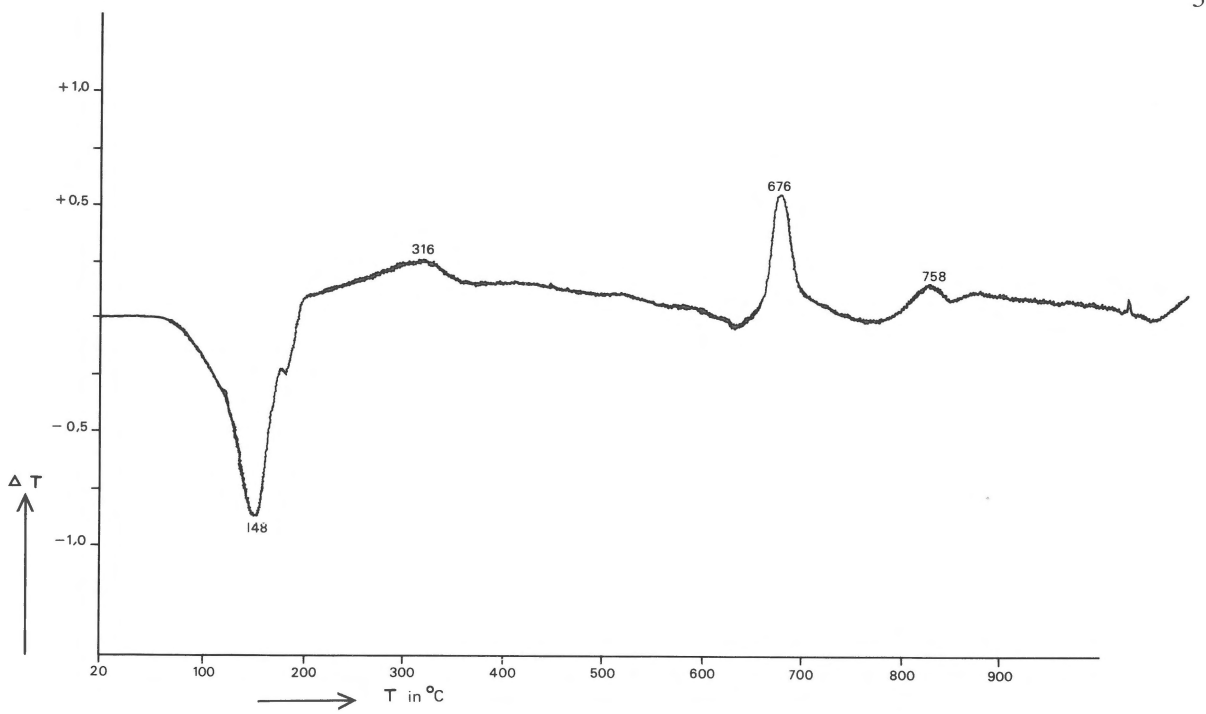

Fig. 5. Differential thermal analytical curve of the Borne vivianite.

The sharp peak at 676° C may be attributed to a structural transformation (Kleber et al., 1965; Pei-lin Tien & Truman C.Waugh, 1969; Henderson et al., 1984). The broad peak at 758° C, which in that temperature range was also observed in several New Zealand vivianites, is considered by Henderson et al. (1984) to result from sintering. To our knowledge the very broad peak at ca. 315° C visible in the Borne curve, has never been reported or discussed elsewhere.

Table 3. Major-element chemistry of a number of individual vivianite nodules, of included vivianite clusters and of one single brown isotropic grain, established by microprobe analyses.

	vivianite nodules (n = 14)		vivianite aggregates (n = 6)		isotropic brown grain
	range of values	average	range of values	average	
CaO	0.05 – 0.13	0.05	0.17 – 0.96	0.36	35.6
MnO	0.00 – 0.06	0.02	0.04 – 0.86	0.30	0.5
MgO	0.00 – 0.07	0.02	0.07 – 0.72	0.26	1.03
K_2O	–	–	0.00 – 0.09	0.04	0.44
SiO_2	0.07 – 0.77	0.37	0.25 – 2.97	1.07	7.59
Al_2O_3	0.05 – 0.36	0.15	0.08 – 1.40	0.47	3.35
P_2O_5	30.1 – 31.9	31.19	30.2 – 32.4	31.58	23.8
FeO Fe_2O_3	48.5 – 51.5	50.21	47.1 – 50.6	48.65	6.58
Na_2O	–	–	–	–	0.77
SO_2	–	–	–	–	0.58

Chemical composition

To obtain more information on the possible presence of non-iron analogues of vivianite we measured the major-element chemistry in several individual vivianite nodules from 14 sites. This was also estimated from 6 vivianite aggregates which are included in the calcareous matrix of the S group granules. Finally the major elements were measured in one specimen of the earlier mentioned brown isotropic framework particles.

The data in Table 3 strongly suggest that the separate nodules as well as the aggregates are exclusively made up of vivianite c.q. meta-vivianite. The compositions of the aggregates in the S group members deviate slightly by containing more Mg, Ca, Mn, Si and Al. These somewhat higher levels might be explained a.o. by their different environment of precipitation. Comparison of the present data with those recently produced by the application of X-ray fluorescent procedures on a number of Quaternary vivianite concretions in New Zealand (Henderson et al., 1984), shows similar contents of Ca, Mg and Mn, whereas Si and Al were hardly detected in these latter ones.

From the single analysis of the isotropic dark brown grain (Table 3), it might be concluded that these isotropic components of the S group members are coprolites or rounded detrital fragments originally derived from phosphorites (compare table 19 in Miller, 1962; table 4.7 in Zimmerle, 1982).

Discussion

X-ray diffraction, DTA and major-chemistry data confirm the visual and optical identification, and provide further evidence that the bulk of the vivianite granules is made up of the monoclinic polymorph; metavivianite could not convincingly be demonstrated, while non-iron analogues appeared to be absent.

Thin-section study and examination of the shape of the gravel- and associated sand-sized vivianite particles (Plate 2F) strongly suggest that the mineral originated inside the till deposit. The initially so striking shape of the vivianite nodules (in strong contrast with the irregular, angular or lobate form of the accompanying vivianite sand-particles) is an artefact, the result of pretreatment washing of the gravel. The distribution of the vivianite particles in the size-spectrum of the till matrix constitutes a further argument in support of an "in situ" formation. Vivianite particles are frequently observed in the gravel and coarse sand fractions, but they are almost lacking in the fine sand and coarse silt. Because the mineral has a specific gravity of 2.68, a detrital supply would have produced a better match of the till matrix size distribution.

The existence of vivianite clusters within the granules of the S group could be considered an argument in favour of residual enrichment of the vivianite. However, the aggregates would most likely not have survived physical desintegration of the S granules, while their liberation from the enclosing rock material by chemical weathering seems unlikely in such an environment. Moreover, the generally higher Ca, Mg, Mn, Si and Al abundances of the aggregates do not support this supposition, nor the fact that in the basal level (sample 114), in spite of the high abundance of the S group members, no vivianite has been found. Nevertheless, it is striking that members of the L group have not been observed at the V group-bearing levels and vice versa (Fig. 2). Since, however, the S granules contain, apart from the vivianite clusters, the only demonstrable P-rich components, i.e. the brown isotropic phosphorite grains, there still seems to be a connection between the granules of the V and the S groups.

On the other hand, although the S granules appear to be the main source of phosphorus, it is only one factor out of many required to produce vivianite-generating conditions in the till. If it was the dominant factor indeed, vivianite could be expected to occur also at the other levels of the till bed, in particular in its lower portion where the S group appears to be abundant.

In conclusion, the individual gravel- and sand-sized vivianite found must be considered to be diagenetic. On the basis of the present data, it is not possible to decide whether they were formed during early diagenesis during accumulation of the till

bed, or in a post-depositional stage, before or after burial of the till bed. The internal structure of the vivianite nodules, which sometimes shows abrupt transitions in crystallinity, suggests that precipitation from the interstitial fluids has occurred in two phases, whereas the nodule dimensions seem to point to the availability of rather large interstices in the till matrix, especially during that second precipitation phase. Additional work has to be done on a greater number of till sections in this area to establish whether the restricted occurrence of authigenic vivianite in it is a common feature. Such a study might further elucidate the problem whether the vivianite is the result of early-diagenetic processes as e.g. has been reported by Emerson & Widmer (1978) in the Greifensee (Switzerland), or that the vivianite originated at a much later post-depositional stage.

Acknowledgements

The Working Group SEM, University of Amsterdam, provided scanning electron microscope facilities. We thank Mr. W.J. Lustenhouwer (WACOM) for the microprobe analyses. D.T.A.-work by E. de Water and X-ray diffraction by B. de Leeuw is gratefully acknowledged. Appreciation is extended to Mr. C. Zeegers for preparing thin- and polished sections, to Mrs. C. Oosterveld, who prepared the drawings, and to Mrs. M.C.G. Keijzer-v.d. Lubbe, who typed the manuscript.

References

Anderson, W.R., B. Stringham & J.A. Whelan. 1962. Secondary phosphates from Bingham, Utah – Am. Mineral., 47: 1303–1309

Barwick, A.R. 1951. Vivianite concretions in Aquia Formation (Middle Eocene), Anne Arundel County, Maryland – Am. Mineral., 36: 629–630

Bray, J.T., O.P. Bricker & B.N. Troup. 1973. Phosphate in interstitial waters of anoxic sediments: oxidation effects during sampling procedures – Science 180: 1362–1363

Dell, C.I. 1973. Vivianite: an authigenic phosphate mineral in Great Lakes sediments – Proc. 16th Conf. Great Lakes Res.: 1027–1028

De Smet, L.A.H. 1962. Het Dollard gebied – Thesis, Landbouw Hogeschool Wageningen: 292 pp

Emerson, S. & G. Widmer. 1978. Early diagenesis in anaerobic lake sediments. II. Thermodynamic and kinetic factors controlling the formation of iron phosphate – Geochim. Cosmochim. Acta 42: 1307–1316

Hearn, P.P., D.L. Parkhurst & E. Callender. 1983. Authigenic vivianite in Potomac river sediments: control by ferric oxyhydroxides – J. Sed. Petrology, 53: 165–177

Henderson, G.S., K.A. Rodgers & V. Cassie. 1983. Diatoms accompanying vivianite from the Auckland Province – New Zealand. J. Geol. Geoph. 26: 309–310

Henderson, G.S., P.M. Black, K.A. Rodgers & P.C. Rankin. 1984. New data on New Zealand vivianite and metavivianite – New Zealand J. Geol. Geoph. 27: 367–378

Kahn, J.S. 1956. The analysis and distribution of the properties of packing in sand size sedements, I. On the measurement of packing in sand stones J. Geol. 64, 385 395

Kleber, W., W. Wilde & M. Frenzel. 1965. The thermal decomposition and oxidation of bivalent iron in vivianite – Chem. Erde 24: 77–93

Miller, H.B. 1962. Sedimentary Petrology. Fourth Rev. Ed. Vol. I

Moore, P.B. 1965a. A structural classification of Fe-Mn orthophosphate hydrates – Am. Mineral. 50: 2052–2062

Moore, P.B. 1965b. The crystal structure of lauerite – Am. Mineral. 50: 1884–1892

Moore, P.B. 1970a. Crystal chemistry of basic iron phosphates – Am. Mineral. 55: 135–176

Moore, P.B. 1970b. A crystal-chemical basis for short transition series orthophosphate and orthoarsenate paragenesis – Neues Jahrb. Mineral Monatsh.: 39–44

Moore, P.B. 1971. The $Fe_3^{2+}(H_2O)_a(PO_4)_2$ homologous series: crystal-chemical relationships and oxidized equivalents – Am. Mineral. 56: 1–17

Nriagu, J.O. 1972. Stability of vivianite and ion-pair formation in the system $Fe_3(PO_4)_2$ – H_3PO_4 – H_2O – Geochim. Cosmochim. Acta 36: 459–470

Nriagu, J.O. & C.I. Dell. 1974. Diagenetic formation of iron phosphates in recent lake sediments – Am. Mineral. 59: 934–946

Pei-lin Tien & Truman C. Waugh. 1969. Thermal and X-ray studies on earthy vivianite in Graneros Shale (Upper Cretaceous), Kansas – Am. Mineral. 54: 1355–1362

Rappol, M. 1983. Glacigenic properties of till – Thesis, University of Amsterdam: 225 pp

Rappol, M. 1984. Till in southeast Drente and the origin of the Hondsrug Complex, The Netherlands – Eiszeitalter u. Gegenwart 34: 7–27

Ritz, C., E.J. Essene & D.R. Peactor. 1974. Metavivianite, a new mineral – Am. Mineral. 59: 896–899

Rodgers, K.A. 1977. Some occurrences of vivianite in the Auckland area – New Zealand. J. Geol. Geoph. 20: 327–334

Rosenquist, I.Th. 1970. Formation of vivianite in Holocene clay sediments – Lithos, 3: 327–334

Shimada, I. & H. Kono. 1971. Earthy vivianite from the Pleistocene lacustrine sediments in the Ozikobe Basin,

Miyagi Prefecture, Japan – The Science Reports of Tahoku University, 3–11: 143–157

Sturman, B.D. & J.A. Mandarino. 1976. Baricite, the magnesium-analogue of vivianite, from Yukon Territory – Can. Mineral. 14: 403–406

Van Baren, J. 1927. De bodem van Nederland – S.L. van Looy, Amsterdam: 1365 pp

Van Bemmelen, J.M. 1896. Over de samenstelling, het voorkomen en de vorming van Sideroze (witte klien) en van Vivianiet in de onderste darglaag der Hoogveenen van Zuidoost Drenthe – Verh. Kon. Akad. Wetensch., 1–3: 3–16

Van Calker, F.J.P. 1885. Diluviales aus der Gegend von Neu-Amsterdam – Zeitschr. der Deutsch. Geol. Ges. Bd XXXVII: 792–803

Van der Meene, E.A. 1984. Weginsnijding "De Lemery" naby Borne – Ontsluitingsrapport 105, R.G.D. district Oost: 17 pp

Zandstra, J.G. 1978. Einführung in die Feinkiesanalyse – Der Geschiebesammler 12: 21–38

Zimmerle, W. 1982. Die Phosphorite des nordwestdeutschen Apt und Alb. – Geol. Jahrb. A65: 159–244

Zwaan, P.C. & G. Kortenbout van der Sluys. 1971. Vivianite crystals from Haren, Noord-Brabant Province, The Netherlands – Scripta Geologica 6: 1–7